

06,07

Effects of Sm³⁺ ions modification on the structure and properties of 0.36(Bi_{1-x}Sm_x)ScO₃-0.64PbTiO₃

© E.G. Guk¹, E.P. Smirnova¹, V.N. Klimov², P.A. Pankratiev¹, N.V. Zaytseva¹, E.E. Mukhin¹

¹ Ioffe Institute,
St. Petersburg, Russia

² Central Research Institute of Structural Materials Prometey, National Research Centre Kurchatov Institute,
St. Petersburg, Russia

E-mail: elrguk@gmail.com

Received July 8, 2025

Revised July 8, 2025

Accepted July 10, 2025

Effect of the modification by Sm³⁺ ions on the properties of the solid solution 0.36(Bi_{1-x}Sm_x)ScO₃-0.64PbTiO₃ (BSSPT) with $x = 0.022, 0.038, 0.056$ was studied. The variants of modification such as stoichiometrical, superstoichiometrical, and excess doping after calcination as well as sintering techniques (one-step, two-step) were performed. The crystal structure, elemental composition, dielectric properties and piezoelectric constant d_{33} were measured. BSSPT is shown to be single-phase and it has a tetragonal ($P4mm$) perovskite structure. The elemental composition of all variants of the synthesized BSSPT ceramics demonstrates the almost identical samarium content, including the Sm³⁺ ion doping into the A sublattice of the ceramics perovskite structure ABO_3 after calcination. The maximum value of the dielectric constant ϵ_m and the corresponding temperature T_m decrease with increasing the Sm³⁺ ion concentration. The obtained maximum d_{33} value was 536 pC/N, which exceeds $d_{33} = 525$ pC/N for unmodified 0.36BiScO₃-0.64PbTiO₃.

Keywords: piezoelectric ceramics, modification, microstructure, dielectric properties, piezoelectric properties.

DOI: 10.61011/PSS.2025.08.62269.192-25

1. Introduction

High-temperature piezoelectric ceramics is required in various fields of science and engineering for operating in extreme temperature conditions. One of the possible application is use of these materials when designing piezoelectric motors within the framework of the ITER project (International Thermonuclear Experimental Reactor). In this case, operating conditions of active elements include presence of thermonuclear plasma with neutron fluence exceeding 10^{19} n/cm² and energy above 0.1 MeV at the temperature 250–300 °C. These requirements are met with a high-temperature piezoceramics 0.36BiScO₃-0.64PbTiO₃ (BSPT) that is situated near a morphotropic phase boundary (MPB). BSPT has one of the highest Curie temperatures (~ 450 °C), thereby determining a range of the operating temperatures up to ~ 300 °C [1,2]. Besides, this ceramics demonstrates a high value of the piezoelectric coefficient d_{33} up 525 pC/N, which is required for effective operation of the piezoelectric motors [3]. The latest studies of the BSPT piezoceramics after effect of radiation that simulates the ITER conditions indicate its radiation resistance [4,5].

As of now, solid solutions with ion substitution both in A- and B-position in a lattice of the ABO_3 perovskite are synthesized and studied. BSPT synthesis was soon followed by many studies of a modification of this ceramics with replacement of both Sc and Ti (B-site in the perovskite lattice), which was properly discussed in many publications.

It included synthesis of various compositions of the ceramics based on the solid solutions both Bi(Sc,Me)O₃-PbTiO₃ as well as BiScO₃-PbMeO₃: Bi(Ga,Sc)O₃-PbTiO₃ [6], Bi(Mg,Sc)O₃-PbTiO₃ [7], Bi(Fe,Sc)O₃-PbTiO₃ [8], BiSc-Pb(Bi,Ti,Zn) [9], BiScO₃-Pb(Mn,Ti)O₃ [10], BiScO₃-Pb(Zn,Nb,Ti)O₃ [11], etc.; and investigation of their piezoelectric properties. The obtained results have shown that most of synthesized compositions demonstrate values of the piezoelectric coefficient d_{33} and the Curie temperature T_C , which are significantly inferior of the unmodified composition of BSPT [12]. In particular, when substituting into the B-site, the piezoelectric coefficient d_{33} and the Curie temperature are in an inversely proportional dependence, i.e. with increase of the Curie temperature the piezoelectric constant decreases and with increase of the piezoelectric constant T_C decreases [12]. For example, after addition Zn²⁺ ions into the BSPT ceramics, the value of d_{33} increased to 490 pC/N, while T_C decreased to 328 °C [9]; whereas in case of introducing multivalent Mn ions ($Mn^{4+} \rightarrow Mn^{3+} \rightarrow Mn^{2+}$) into this ceramics the value of T_C increased from 450 to 468 °C, while d_{33} decreased to 270 pC/N [10].

The A-site in the perovskite-structure compositions is usually occupied by ions with a quite large ionic radius, in particular, ions of rare earth elements (REE). As shown in the study [13–15], the REEs can introduce random fields or bonds that change a cation ordering degree. As a result, doping the lead-containing piezo-

ceramics with rare earth elements leads to the increase of permittivity ϵ , the piezoelectric coefficient d_{33} , the electromechanical coupling coefficient k_p and the elastic constants S . However, for the same reason, reduction of the Curie temperature is observed for any REE-modified lead-containing ceramics [16–19]. Eitel et al. were the first to modify BSPT with lanthanum ions [20]. The authors believe that a donor dopant La^{3+} replaced Pb^{2+} in the A-site, i.e. a BSPLT-composition ceramics was synthesized. In this study, results of doping BSPT with lanthanum showed reduction of the Curie temperature almost by 100 °C (to 365 °C) without significant improvement of the piezoelectric properties ($d_{33} = 465 \text{ pC/N}$). The work [21] describes synthesis of the ceramics of the composition $0.38(\text{Bi}_{1-x}\text{La}_x)\text{ScO}_3\text{-}0.62\text{PbTiO}_3$ (BLSPT), where the ion La^{3+} substitutes in the A-site, as the authors believe, not the lead ion Pb^{2+} , but the bismuth ion Bi^{3+} , which appears to be more probable. And in this case modification with the ions La^{3+} results in shifting T_C for BLSPT towards the low temperatures (440 °C when $x = 0.02$ and 395 °C when $x = 0.06$), wherein the maximum value of the piezoelectric coefficient was 245 pC/N. The study of modification of the BSPT ceramics with the rare earth elements was not limited to the lanthanum ions. The work [22] has investigated dopability of this ceramics with cerium. The synthesized ceramics of the composition $0.36(\text{Bi}_{1-x}\text{Ce}_x)\text{ScO}_3\text{-}0.64\text{PbTiO}_3$ demonstrated stability of the perovskite phase of the modified ceramics only for low value $x = 0.01\text{--}0.02$. Partial replacement of the ion Bi^{3+} with the Ce ion of valence from 2+ to 4+ [22] also shifts T_C towards the lower temperatures.

Significant interest was caused by doping the lead-containing ceramics with samarium. It was shown in the work [16] that during doping the piezoceramics of the composition PbZrTiO_3 (PZT) the ion Sm^{3+} substituted Pb^{2+} in the A-position to form $\text{Pb}_{1-x}\text{Sm}_x\text{ZT}$ (PSZT). With the content of samarium $x = 0.06$, the piezoelectric constant increased from 125 to 172 pC/N, wherein the Curie temperature decreased from 313 to 274 °C. Interest to modification of the ceramics with samarium recently has been abruptly activated, since the studies [17,23] demonstrated that the piezoelectric coefficient d_{33} increased in one and a half - two times in the samarium-doped lead-containing PMN-PT ceramics. As the authors believe, this effect is attributed to the fact the addition of the ion Sm^{3+} into the ceramics PMN-PT creates polar regions, heterogeneity and structural instability therein, which results in inevitable deformation of the lattice. As a result, a higher degree of local structural heterogeneity can lead to improvement of the piezoelectric and dielectric characteristics.

The recent work [24] has successfully doped the ceramics $0.36\text{BiScO}_3\text{-}0.64\text{PbTiO}_3$ with samarium into the A-position with replacement of the ion Bi^{3+} with the ion Sm^{3+} . It obtained quite high values of the effective piezoelectric coefficient (718 pC/N) for the nonpolarized ceramics, which were measured at the applied field of 45 kV/cm. However, the obtained result does not correspond to IEEE Standard

requirements to the piezoceramics parameters [25]. The study [26] has investigated the influence on the phase transition and the electrophysical properties of the textured ceramics $(1-x)(\text{Bi}_{0.97}\text{Sm}_{0.03})\text{ScO}_{3-x}\text{PbTiO}_3$. However, all the studies of this paper were carried out for the same content of samarium and dedicated to searching an optimal ratio of components of the solid solution x , which turned out to be 0.62.

An important factor that affects properties of the lead- and bismuth-containing ceramics is an effect of loss of Bi_2O_3 and PbO during high-temperature synthesis due to their volatility. Evaporation of these oxides causes origination of additional vacancies in the A-site instead of the ions Bi^{3+} and Pb^{2+} already during calcination [27]. We assume that it enables incorporating the samarium ions both at a stage of an initial mixture of oxides as well as after calcination of the unmodified BSPT. The available publications do not take into account these specific features of synthesis of the described solid solution. Besides, it is well known that manufacturing BSPT using a two-step sintering method results in a change of a grain size, thereby significantly affecting the transition temperature, values of permittivity ϵ , the piezoelectric coefficient d_{33} and other parameters [1–3].

The present study is aimed at investigating the composition, the crystal structure, the microstructure and the dielectric properties as well as the piezoelectric coefficient d_{33} of the BSPT ceramics at various methods of samarium doping, namely: 1) stoichiometric modification (incorporation of oxides into the initial mixture as per the composition stoichiometry, including Sm_2O_3); 2) superstoichiometric modification (addition of an excess of Sm_2O_3 to the stoichiometric composition of BSPT); as well as 3) incorporation of the excess of Sm_2O_3 into the calcinated unmodified BSPT. The modification options are studied in combination with the sintering modes: a single-step sintering mode (SSS) and a two-step sintering mode (TSS), as important technological factors that determine the material properties.

2. Experiment

We have studied the ceramics of the composition $0.36(\text{Bi}_{1-x}\text{Sm}_x)\text{ScO}_3\text{-}0.64\text{PbTiO}_3$ (BSSPT), where $x = 0.022, 0.038, 0.056$. In order to study the influence of the approach of incorporation of the ion Sm^{3+} on the BSSPT parameters when $x = 0.022$ the samples for sintering were manufactured by three different ones. The batch No. 1 was produced using a mixture of the oxides Bi_2O_3 , Sm_2O_3 , Sc_2O_3 , PbO and TiO_2 that were taken in a ratio corresponding to the composition of the BSSPT stoichiometric modification for $x = 0.022$. In the batch No. 2, the initial mixture consisted of the oxides Bi_2O_3 , Sc_2O_3 , PbO and TiO_2 that corresponded to the stoichiometric composition of the unmodified BSPT with addition of the excess of Sm_2O_3 into this initial mixture. In the batch No. 3, the composition of the initial mixture for calcination corresponded to the

content of the oxides Bi_2O_3 , Sc_2O_3 , PbO , TiO_2 , which are mixed in a stoichiometric ratio for formation of the BSPT ceramics (for $x = 0$) with further addition of Sm_2O_3 after calcination.

All the oxides were pre-calcinated for 4 h: Sc_2O_3 and TiO_2 at $1000^\circ C$, while Bi_2O_3 and PbO — at $700^\circ C$ due to their volatility. All the three options of the initial mixture of the oxides were milled by grinding a suspension for 24 h and the produced powder was pressed under uniaxial pressure in a mold of the diameter of 2.5 cm at $P = 12$ MPa for calcination in an open platinum crucible at $850^\circ C$ for 4 h. The samples of the batches No. 1 and 2 were taken to form a powder for sintering by 12-hour grinding of their alcohol suspension in a traditional method. Before similarly grinding the samples of the batch No. 3, the composition of the BSPT powder was supplemented for final sintering with samarium oxide Sm_2O_3 in an amount of x that was equal to 2.2 mol%. In all the cases, the formed powder was dried and pressed under uniaxial pressure of $P = 8$ MPa to form disks of the diameter of 10 mm and the thickness of 1 mm, which was followed by separation the disk of each batch into 2 groups: 1a, 2a, 3a, which were sintered in the single-step mode, and 1b, 2b, 3b, which were sintered in the two-step mode. The single-step mode provided for sintering when $T_1 = 1200^\circ C$ for 2 h. The two-step sintering was performed by our designed modified technique [3]: the first step included heating to $T_1 = 1150^\circ C$, switching off a furnace in 1 min after reaching this temperature and cooling to $T_2 = 800^\circ C$ together with the furnace. The second step of sintering was carried out at this temperature for 4 h. In all the cases, an „atmospheric“ pill of lead zirconate was placed near the sample during sintering to compensate for lead losses. A dependence of the parameters of the synthesized BSSPT ceramics on the samarium concentration was studied in a mode that corresponded to the option 1b (the stoichiometric modification, two-step sintering) on the disks of the composition $0.36(Bi_{1-x}Sm_x)ScO_3-0.64PbTiO_3$ when $x = 0, 0.022, 0.038, 0.056$. In all the cases, losses of $PbO + Bi_2O_3$ do not exceed 1 mass.%. Silver was used as a material for electrodes. The electrodes were burned in at the temperature of $500^\circ C$.

The obtained samples were studied in an X-ray diffractometer DRON-3 using radiation of the line $CuK\alpha$, $\lambda = 1.54178$ Å, a Ni-filter and a power supply (38 kV, 18 mA). Scanning was carried out within an interval of the angles 2θ from 10 to 60° with an increment of 0.1°. For measuring lattice parameters, germanium was used as a reference. All the produced samples were single-phase ones and had a perovskite structure. The measured density of the samples was 93–96 % of the theoretical X-ray density.

The elemental composition and the grain sizes of the ceramics were analyzed in a scanning electron microscope TescanMira with a system of elemental composition determination. Dielectric properties were measured using the R5079 AC bridge (the frequency was 1 kHz, the amplitude was 1 V). The samples were polarized at $T = 115^\circ C$ for 30 min in silicon oil in the field $E = 40$ kV/cm applied to

the disk thickness. The piezoelectric coefficient d_{33} was measured on the polarized samples using a displacement indicator of the M-048 model and a high-voltage source produced by Stanford Research Systems. Inc., Model PS350/5000V-25W. We have measured strain that occurred during application of the electric field due to a reverse piezoelectric effect.

3. Results and discussion

X-ray diffraction patterns of the samples of the composition $0.36(Bi_{1-x}Sm_x)ScO_3-0.64PbTiO_3$ ($x = 0, 0.022, 0.038, 0.056$), which are synthesized using various methods of addition of the ion Sm^{3+} , demonstrate a tetragonal ($P4mm$) structure as in the case of the unmodified BSPT composition. The lattice parameters of Table 1 were measured using X-ray diffractometry (XRD) and scanning electron microscopy (SEM) and depend on the modification method.

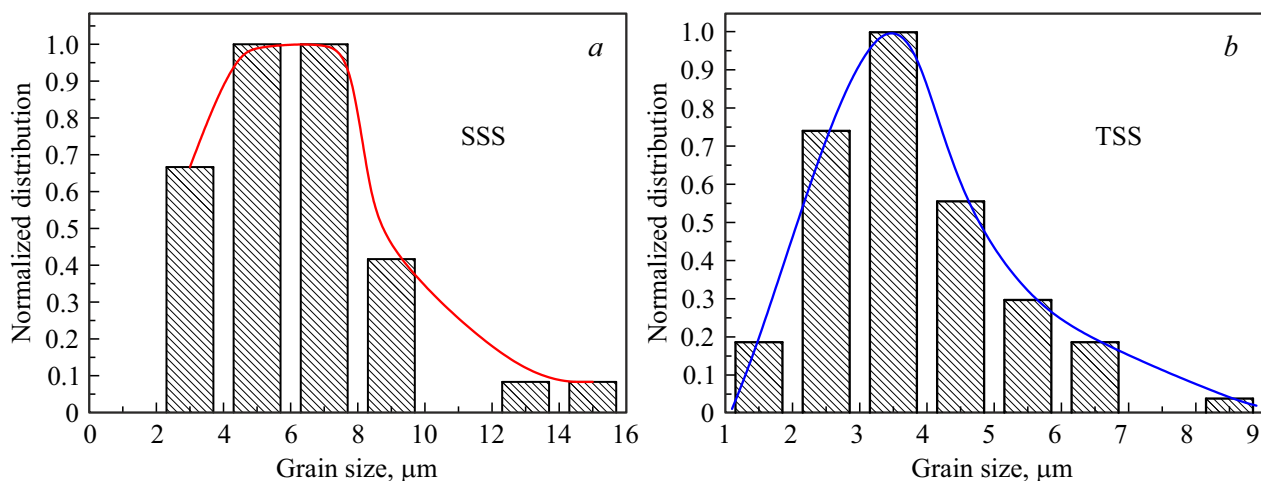
In case of the option No. 1 (the stoichiometric modification) the lattice parameters a and c differ at the various methods of addition of the ion Sm^{3+} and the various synthesis modes, but values of lattice tetragonality are close to each other for all the cases (c/a is within the limits from 1.021 to 1.025). This result differs from data for the unmodified BSPT ceramics, where in a transition from single-step to two-step sintering a lattice tetragonality degree decreases from $c/a = 1.025$ to $c/a = 1.017$, respectively. The superstoichiometric modification (the option No. 2) demonstrates reduction of the lattice tetragonality as compared to the stoichiometric modification. An increase of tetragonality is observed for the modification option No. 3 during synthesis in the SSS mode, so are equal tetragonality degrees for the options No. 2 and No. 3 during the TSS mode. Variations of the tetragonality degree indicate certain differences in a position of the composition near the morphotropic phase boundary (MPB) with preservation of the tetragonal structure.

The elemental composition of the BSSPT-ceramics samples that are synthesized using the various methods and modes of addition of the ion Sm^{3+} , which are listed in Table 1, demonstrate almost the same content of samarium in the synthesized ceramics irrespective both of its incorporation method as well as the synthesis modes (single-step and two-step ones). This result (~ 0.4 wt.%) obtained by SEM in weight % is close to a value of the content of samarium in the final mixture, which is expressed in the same units: 0.4618 wt.% for the stoichiometric modification option and 0.4609 wt.% for the superstoichiometric modification and addition of the excess of Sm_2O_3 after calcination.

Taking into account no feature of the second phase in the obtained X-ray diffraction patterns, it can be concluded that the BSPT ceramics is fully doped with the samarium ions. The described results also indicate that the ions Sm^{3+} can be incorporated into the BSPT lattice after calcination.

Table 1. Influence of the mode and the method of addition of 2.2 mol% of the ion Sm^{3+} into the BSPT composition

Method of measurement and parameters	SSS			TSS		
	Method of addition of Sm		Method of addition of Sm			
	Unmodified BSPT ceramics $c/a = 1.025$ Pb: 42.8 wt.% Bi: 22.5 % $\varepsilon_m = 33092$ $T_m = 450^\circ\text{C}$ $d_{33} = 350 \text{ pC/N}$			Unmodified BSPT ceramics $c/a = 1.017$ Pb: 43.5 wt.% Bi: 23.7 wt.% $\varepsilon_m = 16115$ $T_m = 433^\circ\text{C}$ $d_{33} = 525 \text{ pC/N}$		
	Stoichio-metric modification	Superstoichio-metric modification	Excess in BSPT after calcination	Stoichio-metric modification	Superstoichio-metric modification	Excess in BSPT after calcination
XRD	$a = 3.987 \pm 0.002 \text{ \AA}$ $c = 4.078 \pm 0.002 \text{ \AA}$ $\bar{a} = 4.017 \text{ \AA}$ $c/a = 1.023$	$a = 4.001 \pm 0.003 \text{ \AA}$ $c = 4.080 \pm 0.003$ $\bar{a} = 4.027 \text{ \AA}$ $c/a = 1.0207$	$a = 3.969 \pm 0.002 \text{ \AA}$ $c = 4.073 \pm 0.003$ $\bar{a} = 4.003 \text{ \AA}$ $c/a = 1.025$	$a = 3.979 \pm 0.002$ $c = 4.070 \pm 0.003$ $\bar{a} = 4.009 \text{ \AA}$ $c/a = 1.023$	$a = 3.9900 \pm 0.00$ $c = 4.075 \pm 0.002 \text{ \AA}$ $\bar{a} = 4.019 \text{ \AA}$ $c/a = 1.021$	$a = 3.99 \pm 0.002 \text{ \AA}$ $c = 4.075 \pm 0.002 \text{ \AA}$ $\bar{a} = 4.018 \text{ \AA}$ $c/a = 1.021$
SEM	Pb: 40.2 wt.% Bi: 21.2 wt.% Sm: 0.4 wt.%	Pb: 38.0 wt.% Bi: 22.4 wt.% Sm: 0.3 wt.%	Pb: 41.6 wt.% Bi: 23.0 wt.% Sm: 0.4 wt.%	Pb: 40.5 wt.% Bi: 21.7 wt.% Sm: 0.4 wt.%	Pb: 43.1 % Bi: 24.1 wt.% Sm: 0.4 wt.%	Pb: 44.2 % Bi: 24.2 wt.% Sm: 0.45 wt.%
ε_m	35644	33222	28268	19385	22530	18100
T_m, C°	417.24	415.92	424	407	416	425
$d_{33}, \text{pC/N}$	240	270	250	536	240	400

**Figure 1.** Histograms and functions of grain size distribution of the ceramics $0.36(\text{Bi}_{1-x}\text{Sm}_x)\text{ScO}_3\text{-}0.64\text{PbTiO}_3$, $x = 0.022$, for *a*) the single-step sintering mode and *b*) the two-step sintering mode.

This effect is likely caused by formation of vacancies in the ceramics in the A-site due to high volatility of both Bi_2O_3 and PbO at the temperatures above 800°C similarly, for example, to a process that was observed in the ceramics $\text{Bi}_{1/2}\text{Na}_{1/2}\text{TiO}_3$ (BNT) [28]. Thus, both the X-ray diffraction patterns as well as the results of SEM of the samples of the composition $0.36(\text{Bi}_{1-x}\text{Sm}_x)\text{ScO}_3\text{-}0.64\text{PbTiO}_3$ when $x = 0.022$ indicate that addition of Sm_2O_3 after the calcination step allows incorporating the ions Sm^+ into the BSSPT-ceramics vacancies formed in the A sublattice.

The obtained electronic images were used to construct the histograms of grain-size distribution and their envelope curves for all the synthesized ceramics samples. Figure 1 shows these histograms for the stoichiometric modification of the samarium addition method ($x = 0.022$), which are formed as a result of the single-step sintering mode

(Figure 1, *a*) and the two-step sintering mode (Figure 1, *b*). As can be seen in Figure 1, doping with the samarium ions even at its low concentration ($x = 0.022$) significantly affects the average grain size that is $6\ \mu m$ for the single-step synthesis mode and $3.5\ \mu m$ for the two-step synthesis mode, respectively. Thus, there is still a trend of reduction of the average grain size, which was demonstrated when substituting from single-step to two-step sintering during synthesis of the unmodified BSPT ceramics [2,3].

The decrease of the average grain size when modifying the lead-containing ceramics with REE was observed in the works [16,29], which investigated samarium doping of the PLZT ceramics to form the solid solution $[Pb_{0.925-x}Sm_xLa_{0.075}(Zr_{0.2}Ti_{0.8})_{0.981}O_3]$ and of the PZT ceramics to form the solid solution $[Pb_{1-x}Sm_x(Zr_{0.55}Ti_{0.45})_{1-x/4}O_3]$, which in both the cases was in the single-step sintering mode. The similar result was obtained for the BSPLT ceramics in the work [20], in which sintering was carried out in the single-step sintering mode. It was shown that replacing, presumably, the ion Pb^{2+} with the ion La^{3+} results in reduction of the average grain size from $7.5\ \mu m$ to the value $\leq 1\ \mu m$. The work [12] attempted to explain this fact by compensation of the difference of the charges of lanthanum and lead in the *A* site due to formation of vacancies (V_B) in the *B* site, which complicated motion of grain boundaries, reducing the grain size. At the same time, we believe that it is unjustified to assume that the ion Pb^{2+} is predominantly substituted with the ion La^{3+} to form the vacancies, taking into account that the ions Bi^{3+} can be substituted with the ions La^{3+} . The work [19] describes synthesis and characteristics of the BLSPT ceramics produced by doping the BSPT with lanthanum, as a result of which the ion La^{3+} , as the authors believe, replaces Bi^{3+} that is equal in charge and close in the ionic radius, in the *A*-site, i.e. there is no need to form a vacancy in the *B*-site. It is shown for the ceramics of the BLSPT composition, in which La^{3+} substitutes Bi^{3+} in the *A*-site in the work [21] is shown that modification with lanthanum resulted not in a decrease, but a significant growth of grains despite the fact that the BLSPT was synthesized by the traditional technique with single-step sintering. Results of the study [24] dedicated to investigation of doping the BSPT ceramics with samarium (where the ceramics $0.36(Bi_{1-x}Sm_x)ScO_3-0.64PbTiO_3$ ($x = 0.1, 0.2, 0.3, 0.4, 0.5$) was also synthesized in the traditional technique) indicate that the grain size is increased due to replacing the ions Bi^{3+} with the ions Sm^{3+} during sintering in the SSS mode.

The Figures 2 and 3 show the envelope curves of the normalized function of size distribution of grains for the single-step mode (Figure 2) and the two-step mode (Figure 3) for the BSSPT-ceramics samples ($x = 0.022$) synthesized by the various methods of samarium incorporation. For comparison, the envelope curves for the unmodified BSPT ceramics are given.

The envelope curves of Figure 2 (single-step sintering) demonstrate the increase of the grain sizes as compared

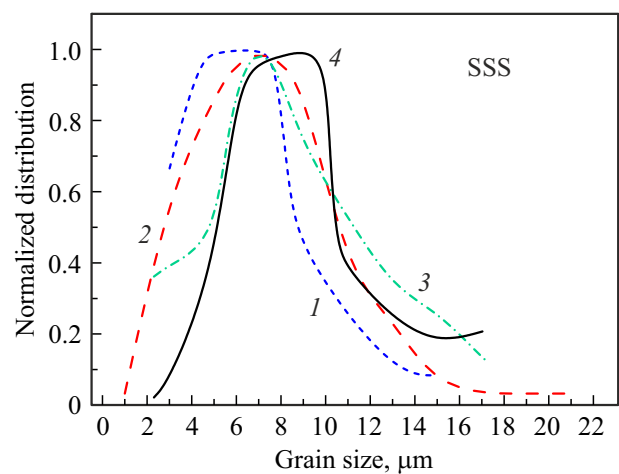


Figure 2. Envelope curves of the normalized function of size distribution of grains for the BSSPT samples ($x = 0.022$) that are produced by the various methods in the single-step sintering mode. The curve 1 — BSSPT, the stoichiometric modification; 2 — BSSPT, the superstoichiometric modification; 3 — BSSPT, the excess of Sm_2O_3 is added to the calcinated BSPT, 4 — the unmodified BSPT.

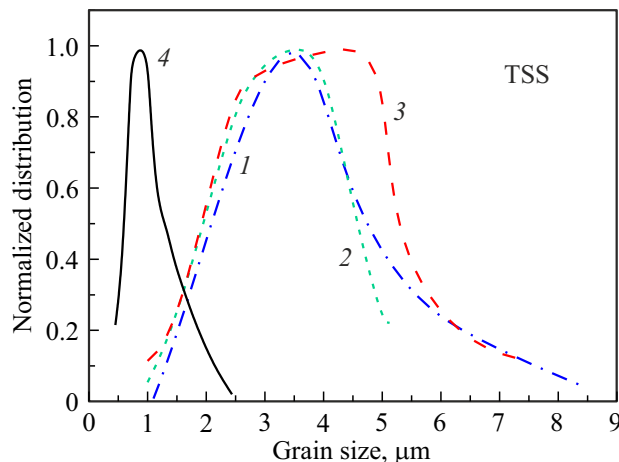


Figure 3. Envelope curves of the normalized function of size distribution of grains for the BSSPT samples ($x = 0.022$) that are produced by the various methods in the two-step sintering mode. The curve 1 — BSSPT, the stoichiometric modification; 2 — BSSPT, the superstoichiometric modification; 3 — BSSPT, the excess of Sm_2O_3 is added to the calcinated BSPT, 4 — the unmodified BSPT.

to the envelopes of Figure 3 (two-step sintering), which corresponds to a pattern of reduction of the grain sizes when substituting from the SSS to TSS mode for the unmodified BSPT ceramics [2,3]. As known, this reduction of the grain sizes is due to freezing of points of grain boundary contact, thereby preventing migration of these boundaries [2].

However, incorporation of the ions Sm^{3+} into BSPT additionally affects process of grain boundary migration, thereby the size of the ceramics grains both in the case of the single-

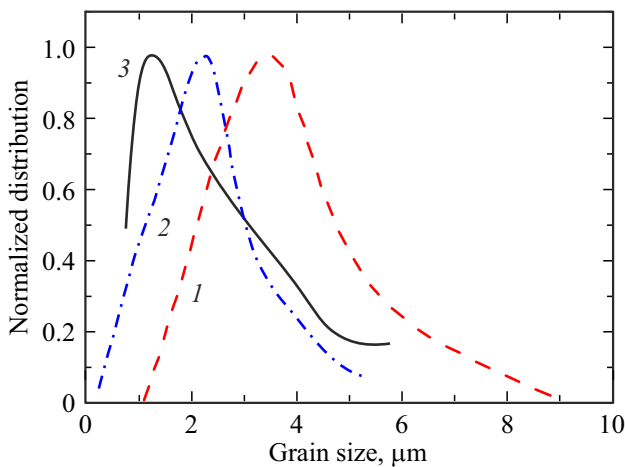


Figure 4. Envelope curves of the normalized function of size distribution of grains in the ceramics $0.36(\text{Bi}_{1-x}\text{Sm}_x)\text{ScO}_3\text{-}0.64\text{PbTiO}_3$ for the various concentrations: the curve 1 — $x = 0.022$; 2 — $x = 0.038$; 3 — $x = 0.056$.

step sintering mode and of the two-step sintering mode as well. As follows from Figure 2, in case of the single-step mode of synthesis of $0.36(\text{Bi}_{1-x}\text{Sm}_x)\text{ScO}_3\text{-}0.64\text{PbTiO}_3$ all the envelope curves for this ceramics when $x = 0.022$ demonstrate reduction of the average grain size in 1.5–2 times (i.e. 5–7 μm as compared to 10 μm for the undoped BSPT ceramics). Addition of samarium into the ceramics causes local stresses due to a difference of radii of the ion Bi^{3+} and the ion Sm^{3+} that substitutes it, thereby resulting in the change of the cation ordering degree [13–15] and reducing grain boundary migration and, therefore, the average grain size. In case of transiting to the two-step mode of incorporation of the ions Sm^{3+} into BSPT (Figure 3), not so great reduction of the grain sizes as compared to the unmodified ceramics is observed (3.5–4.5 μm as compared to 0.88 μm). The increase of the concentration of the ion Sm^{3+} in the modified ceramics $0.36(\text{Bi}_{1-x}\text{Sm}_x)\text{ScO}_3\text{-}0.64\text{PbTiO}_3$ demonstrates further reduction of the grain size (Figure 4) due to further attenuation of a mobility limitation and deceleration of grain boundary motion [12].

Thus, in each specific case the grain size is determined by a balance of the processes of grain boundary migration and deceleration of motion of these boundaries as well as limitation of mobility. As a result, when transiting from the single-step to two-step sintering mode, traditional reduction of the grain size is observed, but this reduction is attenuated. Discrepant data on a microstructure of the BSPT ceramics when doping with samarium, which are obtained in the present study and a paper [24] indicate that it is necessary to further investigate mechanisms that determine the grain growth and their distribution.

Table 1 shows results of measurement of the temperature dependence of permittivity ε at the frequency of 1 kHz for the various modes and methods of incorporation of 2.2 mol% Sm into the BSPT composition. As in the case

of the unmodified BSPT ceramics [30], for the samples synthesized in the single-step sintering mode, values of a real part of permittivity ε_m in the maximum in 1.5–2 times exceed these parameters obtained in the two-step mode, which is likely primarily due to a smaller grain size in the ceramics formed in the TSS mode. For example, for the case of stoichiometric modification of the BSSPT with samarium when $x = 2.2$ mol% the value of permittivity in the maximum is $\varepsilon_m = 35644$ in the SSS mode, while $\varepsilon_m = 19385$ in the TSS mode *ceteris paribus*. Many studies are dedicated to studying the influence of the grain size on permittivity of the piezoceramics. This issue is discussed in detail using barium titanate as an example in the review [31], which discusses main mechanisms of this influence: internal stress [32], a contribution by 90° domains [33] and a contribution by areas of interphase grain boundaries [34]. It is shown that depending on the grain size the ceramics can be divided into 3 groups: 1) a group with the grain size from 10 to 50 μm , in which an internal stress that originates during the phase transition is reduced as a result of twinning of the 90° domains; 2) a group of the grain size $< 10 \mu\text{m}$, where the width of the 90° domains decreases in proportion to a square root of the grain diameter [35], which can be explained by equilibrium of an elastic-field energy and a domain-wall energy. The smaller the grain size, the higher the contribution by the 90° domain walls to dielectric and elastic constants. When the grain size exceeds 1 μm , the width of the 90° domain decreases with a decrease of the grain size, thereby resulting in higher activity of the 90° of domain-walls and improvement of the piezoelectric properties [36]. The third group, which is the ceramics with an ultrafine grain ($< 1 \mu\text{m}$), exhibits an increase of the contribution by the areas of the interphase grain boundaries with a low value of permittivity to a significant percentage [37]. As a result, the grain boundary increases as

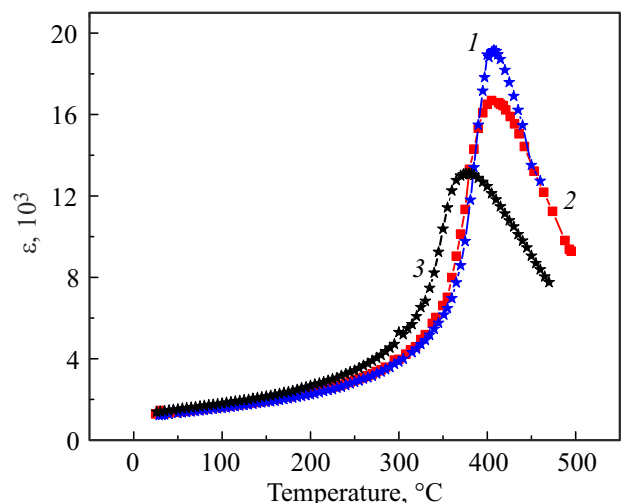
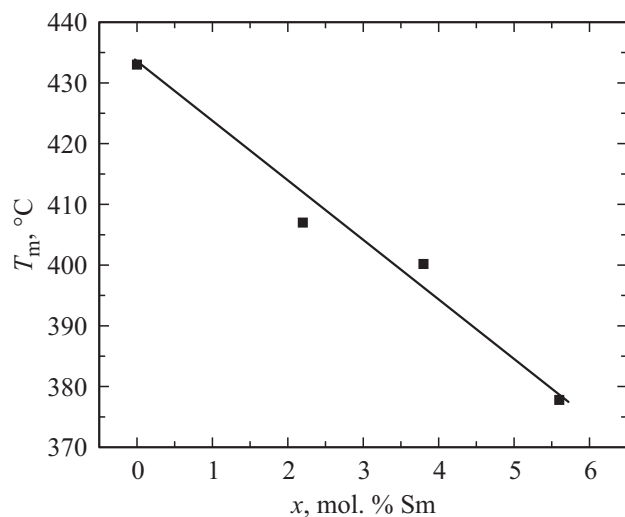


Figure 5. Dependence of permittivity ε on the temperature for the ceramics $0.36(\text{Bi}_{1-x}\text{Sm}_x)\text{ScO}_3\text{-}0.64\text{PbTiO}_3$ with the various Sm concentration: the curve 1 — $x = 0.022$, 2 — $x = 0.038$, 3 — $x = 0.056$.

Table 2. Influence of the value of the Sm concentration on the parameters of the BSSPT ceramics

Parameter	TSS, the stoichiometric modification			
	Sm concentration (x), mol.%/wt.%			
	0/0	2.2/0.4618	3.8/0.797	5.6/1.1521
XRD	$a = 3.995 \pm 0.004 \text{ \AA}$ $c = 4.064 \pm 0.004 \text{ \AA}$ $c/a = 1.017$	$a = 3.979 \pm 0.002 \text{ \AA}$ $c = 4.070 \pm 0.003 \text{ \AA}$ $\bar{a} = 4.009 \text{ \AA}$ $c/a = 1.023$	$a = 3.988 \pm 0.002 \text{ \AA}$ $c = 4.076 \pm 0.002$ $\bar{a} = 4.009 \text{ \AA}$ $c/a = 1.022$	$a = 3.992 \pm 0.002 \text{ \AA}$ $c = 4.070 \pm 0.003 \text{ \AA}$ $\bar{a} = 4.018 \text{ \AA}$ $c/a = 1.019$
SEM	Pb: 43.5 Bi: 23.7	Pb: 40.5 Bi: 21.7 Sm: 0.4	Pb: 40.0 Bi: 22.4 Sm: 0.9	Pb: 43.5 Bi: 23.4 Sm: 1.6
ϵ_m	16000	19385	18776.3	13078.87
$T_m, ^\circ\text{C}$	433	407	400.17	377.78
$d_{33}, \text{pC/N}$	525	536	275	270

**Figure 6.** Dependence of the temperature that corresponds to the maximum value of permittivity ϵ_m , on the concentration of the ions Sm^{3+} .

the grain size decreases, therefore, a motion of the domain wall is heavily limited and the external effect decreases. Thus, as the authors believe, optimal dielectric parameters shall be observed in the piezoceramics with the average grain size ($> 1 \mu\text{m}$, but $< 10 \mu\text{m}$), but for the specific compositions of the piezoceramics, with preservation of the described trend these boundaries have specific values that depend on the composition of the ceramics and its structure.

The value of permittivity in the maximum ϵ_m and its respective temperature T_m decrease with an increase of the concentration of the ions Sm^{3+} in the composition of the ceramics. Figure 5 shows the temperature dependences of permittivity ϵ of the ceramics synthesized at the stoichiometric modification in the two-step mode, for the various concentrations of the ion Sm^{3+} .

It follows from Figure 6, which shows the dependence of the temperature T_m on the concentration of the ion Sm^{3+} , that the value of T_m almost linearly decreases with the increase of the concentration of Sm^{3+} .

It follows from the data of the tables 1 and 2 that the piezoelectric constant d_{33} has a value $\sim 400 \text{ pC/N}$ for the BSSPT ceramics that is produced as a result of the two-step sintering mode at the stoichiometric modification and when incorporating the excess of samarium after calcination.

For the option of the stoichiometric modification, the maximum value of d_{33} achieves 536 pC/N, which exceeds the value 525 pC/N for the unmodified BSPT.

4. Conclusions

We have studied the options of modification of the ceramics $0.36\text{BiScO}_3\text{-}0.64\text{PbTiO}_3$ (BSPT) with the ions Sm^{3+} : 1) the stoichiometric modification, 2) the superstoichiometric modification, 3) incorporation of the excess of $Sm_2\text{O}_3$ into the unmodified calcinated BSPT in combination with the two sintering modes (the single-step one, the two-step one). We have synthesized the ceramics of the composition $0.36(\text{Bi}_{1-x}\text{Sm}_x)\text{ScO}_3\text{-}0.64\text{PbTiO}_3$ (BSSPT), where $x = 0.022, 0.038, 0.056$. The X-ray diffraction patterns of the synthesized BSSPT samples demonstrate the tetragonal ($P4mm$) structure.

The elemental composition of all the options of the synthesized samples of the BSSPT ceramics is studied to show almost the same content of samarium. The results obtained in the present study indicate that it is possible to incorporate the ions Sm^{3+} into the BSPT lattice both during superstoichiometric incorporation and introduction after calcination.

The grain size distribution histograms, which are constructed based on the obtained electronic images, confirm that doping with the samarium ions even at its low

concentration ($x = 0.022$) significantly affects the grain size. When transiting from the single-step sintering mode to the two-step mode, there is traditional reduction of the grain sizer, but this reduction is attenuated by incorporation of the samarium ions. As a result, in the case of the single-step synthesis, modification with the ions Sm^{3+} results in reduction of the grain sizes in 1.5–2 times (from 10 to $5\text{--}7\ \mu\text{m}$), while in the case of the two-step synthesis there is an increase of the grain size from 0.88 to 3.5–4.5 μm , which corresponds to the dependence obtained for the unmodified BSPT ceramics [3].

The results of measurement of the temperature dependence of permittivity demonstrate reduction of both the value of permittivity in the maximum ϵ_m and the value of its respective temperature T_m when transiting from single-step to two-step sintering for the various methods of incorporation of the ions Sm^+ into the BSPT composition. The value of the temperature T_m linearly decreases with the increase of the concentration of the ions Sm^+ . The value of d_{33} , which is obtained in the present study, achieves 536 pC/N, which exceeds $d_{33} = 525$ pC/N for the unmodified BSPT.

Conflict of interest

The authors declare that they have no conflict of interest.

References

- [1] R.E. Eitel, C.A. Randall, T.R. Shrout, S.-E. Park. *Jpn. J. Appl. Phys.* **41**, 4R, 2099 (2002).
- [2] T. Zou, X. Wang, W. Zhao, L. Li. *J. Am. Ceram. Soc.* **9**, 1, 121 (2008).
- [3] E.G. Guk, E.P. Smirnova, V.N. Klimov, P.A. Pankrat'ev, N.V. Zaitseva, A.V. Sotnikov, E.E. Mukhin. *FTT* **66**, 8, 1397 (2024). (in Russian).
- [4] E.P. Smirnova, V.N. Klimov, E.G. Guk, P.A. Pankrat'ev, N.V. Zaitseva, A.V. Sotnikov, E.E. Mukhin. *FTT* **65**, 11, 1971 (2023). (in Russian).
- [5] E.P. Smirnova, V.N. Klimov, E.G. Guk, P.A. Pankrat'ev, N.V. Zaitseva, A.V. Sotnikov, E.E. Mukhin. *FTT* **66**, 1, 103 (2024). (in Russian).
- [6] J. Cheng, R. Eitel, N. Li, L.E. Cross. *J. Appl. Phys.* **94**, 1, 605 (2003).
- [7] Q. Zhang, Z. Li, F. Li, Z. Xu, X. Yao. *J. Am. Ceram. Soc.* **93**, 10, 3330 (2010).
- [8] I. Sterianou, D.C. Sinclair, I.M. Reaney, T.P. Comyn, A.J. Bell. *J. Appl. Phys.* **106**, 8, 084107 (2009).
- [9] Y. Dong, K. Zhao, Z. Zhou, R. Wang. *J. Am. Ceram. Soc.* **105**, 11, 6898 (2022).
- [10] S.J. Zhang, R.E. Eitel, C.A. Randall, T.R. Shrout, E.F. Alberta. *Appl. Phys. Lett.* **86**, 26, 262904 (2005).
- [11] Z. Yao, H. Liu, M. Cao, H. Hao, Z. Yu. *Mater. Res. Bull.* **46**, 8, 1257 (2011).
- [12] Y. Dong, K. Zou, R. Liang, Z. Zhou. *Prog. Mater. Sci.* **132**, 101026 (2023).
- [13] J. Chen, H.M. Chan, M.P. Harmer. *J. Am. Ceram. Soc.* **72**, 4, 593 (1989).
- [14] G.A. Samara. *J. Phys. Condens. Matter* **15**, 9, R367 (2003).
- [15] W. Kleemann. *Physica Status Solidi B* **251**, 10, 1993 (2014).
- [16] S.K. Pandey, O.P. Thakur, D.K. Bhattacharya, C. Prakash, R. Chatterjee. *J. Alloys. Compd.* **468**, 12, 356 (2009).
- [17] C. Li, B. Xu, D. Lin, S. Zhang, L. Bellaiche, T.R. Shrout, F. Li. *Phys. Rev. B* **101**, 14, 140102(R) (2020).
- [18] H. Zhou, S. Yang, Z. Xi, S. Dong, F. Guo, W. Long, X. Li, P. Fang, Z. Dai. *J. Mater. Sci.* **56**, 21, 12121 (2021).
- [19] Z. Fang, X. Tian, F. Zheng, X. Jiang, W. Ye, Y. Qin, X. Wang, Y. Zhang. *Ceram. Int.* **48**, 6, 7550 (2022).
- [20] R.E. Eitel, T.R. Shrout, C.A. Randall. *Jpn. J. Appl. Phys.* **43**, 12, 8146 (2004).
- [21] Y. Chen, D. Lan, Q. Chen, Z. Xu, X. Yue, D. Xiao, J. Zhu. *Mater. Res. Soc. Symp. Proc.* **888**, 1, - (2006).
- [22] Y. Chen, Y. Ma, D. Xue, J. Zhu. „Piezoelectric Ceramics“ Int. Conf. on Materials Engineering and Information Technology Applications (MEITA), 853 (2015).
- [23] F. Li, D. Lin, Z. Chen, Z. Cheng, J. Wang, C. Li, Z. Xu, Q. Huang, X. Liao, L.-Q. Chen, T.R. Shrout, S. Zhang. *Nature Mater.* **17**, 4, 349 (2018).
- [24] S.W. Cho, J.M. Baik, Y.H. Jeong. *Ceram. Int.* **49**, 2, 1865 (2023).
- [25] IEEE Standard on Piezoelectricity. ANSI/IEEE Std 176–1987. Institute of Electrical and Electronics Engineers Inc., New York (1987).
- [26] M.-S. Lee, Y.H. Jeong. *Ceram. Int.* **49**, 23, 37936 (2023).
- [27] J.-H. Ji, D.-J. Shin, J. Kim, J.-H. Koh. *Ceram. Int.* **46**, 4, 4104 (2020).
- [28] X.X. Wang, X.G. Tang, K.W. Kwok, H.L.W. Chan, C.L. Choy. *Appl. Phys. A* **80**, 5, 1071 (2005).
- [29] P. Singh, S. Singh, J.K. Juneja, K.K. Raina, R.P. Pant, C. Prakash. *Integrated Ferroelectrics* **122**, 1, 23 (2010).
- [30] P.A. Pankrat'ev, E.P. Smirnova, V.N. Klimov, E.G. Guk, N.V. Zaitseva, A.V. Sotnikov, E.E. Mukhin. *FTT* **67**, 3, 514 (2025). (in Russian).
- [31] H. Ghayour, M. Abdellahi. *Powder Technol.* **292**, 84 (2016). <https://doi.org/10.1016/j.powtec.2016.01.030>
- [32] W.R. Buessem, L.E. Cross, A.K. Goswami. *J. Am. Ceram. Soc.* **49**, 1, 34 (1966).
- [33] G. Arlt, D. Hennings, G. de With. *J. Appl. Phys.* **58**, 4, 1619 (1985).
- [34] M.H. Frey, Z. Xu, P. Han, D.A. Payne. *USA Ferroelectrics* **206**, 1, 337 (1998).
- [35] W. Cao, C.A. Randall. *J. Phys. Chem. Solids* **57**, 10, 1499 (1996).
- [36] M. Demartin, D. Damjanovic. *Appl. Phys. Lett.* **68**, 21, 3046 (1996).
- [37] Z. Zhao, V. Buscaglia, M. Viviani, M.T. Buscaglia, L. Mitorseriu, A. Testino, M. Nygren, M. Johnsson, P. Nanni. *Phys. Rev. B* **70**, 2, 024107 (2004).

Translated by M.Shevlev